

Supplementary Table 1 – Strain List

strain	genotype	reference
W303	<i>leu2-3,112 trp1-1 can1-100 ura3-1 ade2-1 his3-11,15 [phi⁺]</i>	(Rothstein, 1983)
56	<i>rad9::HIS3</i>	(de la Torre-Ruiz et al., 1998)
YLL476.34/2C	<i>MEC1-9HA::LEU2::mec1</i> (internal tag)	(Paciotti et al., 2000)
YLL447.32/1A	<i>MEC1-18MYC::LEU2::mec1</i> (internal tag)	(Paciotti et al., 2000)
YBP61	<i>RAD9-9myc::hph-NT1</i>	this study
YBP63	<i>DDC2-9myc::KanMx4</i>	this study
YBP74	<i>URA3::pGAL SIC1 RAD9-9myc::hph-NT1</i>	this study
YBP82	<i>dpb11ΔC::hph-NT1</i>	this study
YBP109	<i>dot1::KanMx4</i>	this study
YBP110	<i>dpb11ΔC::hph-NT1 dot1::KanMx4</i>	this study
YBP162	<i>dpb11::HIS3Mx4 dpb11-WG700,701AA</i>	this study
YBP167	<i>dpb11::HIS3Mx4 dpb11-WG700,701AA dot1::KanMx4</i>	this study
YBP198	<i>rad9ΔN3 451-C-9myc::HIS3Mx6::NAT-NT2</i>	this study
YBP234	<i>TRP1::DPB11ΔN</i>	this study
YBP235	<i>TRP1::DPB11ΔN dot1::KanMx4</i>	this study
YBP236	<i>TRP1::DPB11ΔN dpb11ΔC::hph-NT1</i>	this study
YBP237	<i>TRP1::DPB11ΔN dot1::KanMx4 dpb11ΔC::hph-NT1</i>	this study
YBP242	<i>TRP1::DPB11</i>	this study
YBP243	<i>TRP1::DPB11 dot1::KanMx4</i>	this study
YBP244	<i>TRP1::DPB11 dpb11ΔC::hph-NT1</i>	this study
YBP245	<i>TRP1::DPB11 dot1::KanMx4 dpb11ΔC::hph-NT1</i>	this study
YBP260	<i>pep4::HIS3 RAD9ΔC3 1-750-9myc::hph-NT1</i>	this study
YBP261	<i>pep4::HIS3 RAD9ΔC4 1-540-9myc::hph-NT1</i>	this study
YBP262	<i>pep4::HIS3 RAD9ΔC5 1-450-9myc::KanMx4</i>	this study
YBP263	<i>rad9ΔN7 471-C-9myc::KanMx4::NAT-NT2</i>	this study
YBP264	<i>rad9ΔN8 540-C-9myc::KanMx4::NAT-NT2</i>	this study
YBP269	<i>ddc1-T602A::HIS3Mx6</i>	this study
YBP270	<i>ddc1-T602A::HIS3Mx6 dot1::KanMx4</i>	this study
YBP271	<i>ddc1-T602A::HIS3Mx6 dpb11ΔC::hph-NT1</i>	this study
YBP272	<i>ddc1-T602A::HIS3Mx6 dot1::KanMx4 dpb11ΔC::hph-NT1</i>	this study
YBP278	<i>TRP1::DPB11 T12A dot1::KanMx4 dpb11ΔC::hph-NT1</i>	this study
YBP297	<i>rad9::NAT-NT2 TRP1::RAD9</i>	this study
YBP298	<i>rad9::NAT-NT2 TRP1::RAD9 dot1::KanMx4</i>	this study
YBP299	<i>rad9::NAT-NT2 TRP1::RAD9 dpb11ΔC::hph-NT1</i>	this study
YBP300	<i>rad9::NAT-NT2 TRP1::RAD9 dot1::KanMx4 dpb11ΔC::hph-NT1</i>	this study
YBP301	<i>rad9::NAT-NT2 TRP1::rad9 ST462,474AA</i>	this study
YBP302	<i>rad9::NAT-NT2 TRP1::rad9 ST462,474AA dot1::KanMx4</i>	this study
YBP303	<i>rad9::NAT-NT2 TRP1::rad9 ST462,474AA dpb11ΔC::hph-NT1</i>	this study
YBP304	<i>rad9::NAT-NT2 TRP1::rad9 ST462,474AA dot1::KanMx4 dpb11ΔC::hph-NT1</i>	this study

strain	genotype	reference
YBP305	<i>TRP1::pDPB11 rad9-ST462,474AA-dpb11ΔN</i>	this study
YBP347	<i>rad9::NAT-NT2 TRP1::RAD9-3Flag::HIS3Mx6</i>	this study
YBP349	<i>rad9::NAT-NT2 TRP1::rad9 ST462,474A-3Flag::HIS3Mx6</i>	this study
YBP351	<i>rad9::NAT-NT2 TRP1::rad9 ST462,474A-3Flag::HIS3Mx6 dot1::KanMx4</i>	this study
YBP353	<i>dpb11::HIS3MX4 TRP1::dpb11-1</i>	this study
YBP354	<i>dpb11::HIS3MX4 TRP1::dpb11-1 dot1::KanMx6</i>	this study
YBP358	<i>ddc1::hph-NT1 pRS314 DDC1</i>	this study
YBP359	<i>ddc1::HIS3Mx6 dot1::KanMx4 pRS314 DDC1</i>	this study
YBP360	<i>ddc1::HIS3Mx6 dpb11ΔC::hph-NT1 pRS314 DDC1</i>	this study
YBP361	<i>ddc1::HIS3Mx6 dot1::KanMx4 dpb11ΔC::hph-NT1 pRS314 DDC1</i>	this study
YBP362	<i>ddc1::hph-NT1 pRS314 ddc1 WW352,544AA</i>	this study
YBP363	<i>ddc1::HIS3Mx6 dot1::KanMx4 pRS314 ddc1 WW352,544AA</i>	this study
YBP364	<i>ddc1::HIS3Mx6 dpb11ΔC::hph-NT1 pRS314 ddc1 WW352,544AA</i>	this study
YBP365	<i>ddc1::HIS3Mx6 dot1::KanMx4 dpb11ΔC::hph-NT1 pRS314 ddc1 WW352,544AA</i>	this study
YBP366	<i>rad9::NAT-NT2 TRP1::RAD9-3Flag::HIS3Mx6 pep4::hph-NT1</i>	this study
YBP367	<i>rad9::NAT-NT2 TRP1::rad9 ST462,474A-3Flag::HIS3Mx6 pep4::hph-NT1</i>	this study
YBP370	<i>rad9::NAT-NT2 TRP1::rad9 ST462,474A-3Flag::HIS3Mx6 ddc1-T602A::HIS3Mx6</i>	this study
YBP371	<i>rad9::NAT-NT2 TRP1::rad9 ST462,474A-3Flag::HIS3Mx6 ddc1-T602A::HIS3Mx6 dot1::KanMx4</i>	this study
YBP372	<i>rad9::NAT-NT2 TRP1::pDPB11 rad9-ST462,474AA-dpb11ΔN</i>	this study
YBP373	<i>rad9::NAT-NT2 TRP1::pDPB11 rad9-ST462,474AA-dpb11ΔN dot1::KanMx4</i>	this study
YBP374	<i>rad9::NAT-NT2 TRP1::pDPB11 rad9-ST462,474AA-dpb11ΔN dpb11ΔC::hph-NT1</i>	this study
YBP375	<i>rad9::NAT-NT2 TRP1::pDPB11 rad9-ST462,474AA-dpb11ΔN dot1::KanMx4 dpb11ΔC::hph-NT1</i>	this study
YBP376	<i>rad9::NAT-NT2 TRP1::pDPB11 rad9-ST462,474AA-dpb11ΔNΔC</i>	this study
YBP377	<i>rad9::NAT-NT2 TRP1::pDPB11 rad9-ST462,474AA-dpb11ΔNΔC dot1::KanMx4</i>	this study
YBP378	<i>rad9::NAT-NT2 TRP1::pDPB11 rad9-ST462,474AA-dpb11ΔNΔC dpb11ΔC::hph-NT1</i>	this study
YBP379	<i>rad9::NAT-NT2 TRP1::pDPB11 rad9-ST462,474AA-dpb11ΔNΔC dot1::KanMx4 dpb11ΔC::hph-NT1</i>	this study
YBP381	<i>rad9::NAT-NT2 TRP1::RAD9-3Flag::HIS3Mx6 dpb11ΔC::hph-NT1</i>	this study
YBP383	<i>rad9::NAT-NT2 TRP1::rad9-ST462,474AA-3Flag::HIS3Mx6 dpb11ΔC::hph-NT1</i>	this study
YBP384	<i>rad9::NAT-NT2 TRP1::rad9-ST462,474AA-3Flag::HIS3Mx6 dot1::KanMx4 dpb11ΔC::hph-NT1</i>	this study
YBP395	<i>rad9::NAT-NT2 TRP1::pDPB11 rad9-ST462,474AA-dpb11ΔN dot1::KanMx4 ddc1-T602A::HIS3Mx6</i>	this study
YBP396	<i>rad9::NAT-NT2 TRP1::pDPB11 rad9-ST462,474AA-dpb11ΔN dpb11ΔC::hph-NT1 ddc1-T602A::HIS3Mx6</i>	this study

strain	genotype	reference
YBP397	<i>rad9::NAT-NT2 TRP1::pDPB11 rad9-ST462,474AA-dpb11ΔN dot1::KanMx4 dpb11ΔC::hph-NT1 ddc1-T602A::HIS3Mx6</i>	this study
YBP398	<i>rad9::NAT-NT2 TRP1::pDPB11 rad9-ST462,474AA-dpb11ΔNΔC ddc1-T602A::HIS3Mx6</i>	this study
YBP399	<i>rad9::NAT-NT2 TRP1::pDPB11 rad9-ST462,474AA-dpb11ΔNΔC dot1::KanMx4 ddc1-T602A::HIS3Mx6</i>	this study
YBP400	<i>rad9::NAT-NT2 TRP1::pDPB11 rad9-ST462,474AA-dpb11ΔNΔC dpb11ΔC::hph-NT1 ddc1-T602A::HIS3Mx6</i>	this study
YBP401	<i>rad9::NAT-NT2 TRP1::pDPB11 rad9-ST462,474AA-dpb11ΔNΔC dot1::KanMx4 dpb11ΔC::hph-NT1 ddc1-T602A::HIS3Mx6</i>	this study
PJ69-7A	<i>ura3-52 his3-200 leu2-3,112 trp1-901 ade2 gal4Δ gal80Δ LYS2::pGAL1-HIS3 pGAL2-ADE2 met2::pGAL7-lacZ</i>	(James et al., 1996)

With the exception of PJ69-7A, all strains are W303 background. All strains are MATa.

Supplementary table 2 – Plasmid list

plasmid	vector	insert	reference
1678	pet21b	DPB11	this study
pBP46	pGex4T1	DPB11	this study
pBP48	pGex4T1	DPB11 1-275	this study
pBP60	pGex4T1	DPB11 276-600	this study
pBP44	pGex4T1	DPB11 555-C	this study
pBP55	pGex4T1	DPB11 1-600	this study
pBP62	pGex4T1	dpb11 555-C WG700,701AA	this study
pBP72	pGex4T1	dpb11 555-C W700A	this study
pBP74	pGex4T1	dpb11 555-C G701A	this study
pBP75	pGex4T1	dpb11 555-C TS698,699AA	this study
pBP77	pGex4T2	dpb11 555-C YG735,736AA	this study
pBP57	Yiplac204	pDPB11 DPB11 tADH	this study
pBP84	Yiplac204	pDPB11 dpb11-1 tADH	this study
pBP66	Yiplac204	pDPB11 dpb11 WG700,701AA tADH	this study
pBP93	Yiplac204	pDPB11 DPB11 276- C tADH	this study
pBP66	Yiplac204	pDPB11 dpb11 T11A tADH	this study
pBP89	pYM-N1	pYM- pRAD9::KanMx4	this study
pBP90	pYM-N1	pYM-pRAD9::nat- NT2	this study
pBP91	pMAL c2x	RAD9	this study
pBP113	pMAL c2x	rad9 ST462,474AA	this study
pBP115	pMAL c2x	rad9 SS494,507AA	this study
pBP92	Yiplac204	pRAD9 RAD9 tRAD9	this study
pBP109	Yiplac204	pRAD9 RAD9 ST462,474AA tRAD9	this study
pBP120	Yiplac204	pDPB11 Rad9 ST462,474AA- Dpb11 276-C	this study
pBP121	Yiplac204	pDPB11 Rad9 ST462,474AA- Dpb11 276-600	this study
pBP131	pMAL TEV-His-Flag	RAD9	this study
pBD26	pGBD-C1	DPB11 1-276	this study
pAD25	pGAD-C1	RAD9	this study
pAD27	pGAD-C1	rad9 ST462,474AA	this study
pAD28	pGAD-C1	rad9 S462A	this study
pAD29	pGAD-C1	rad9 T474A	this study

Supplementary table 3 – Antibody list

antibody	organism	Clone/ Number	source
anti-myc	mouse	4A6	Milipore
anti-HA	mouse	16B12	Covance
anti-GST-HRP	rabbit	Z5	Santa Cruz
anti-Flag-HRP	mouse	M2	Sigma
anti-Dpb11-C	rabbit	BPF19	J. Diffley
anti-Rad53	rabbit	JDI48	J. Diffley
anti-Rad9	rabbit		N. Lowndes
anti-Gal4 AD	mouse	C10	Santa Cruz
anti-Rad9 S462	rabbit	BPF23	J. Diffley
anti-Rad9 T474	rabbit	BPF25	J. Diffley
anti-PHAS1	rabbit	PHAS1/ 4EBP1	Cell Signalling
anti-PSTAIRE	mouse	PSTAIRE	Sigma

Supplementary Methods:

Protein purification:

Dpb11-His:

BL21 DE3 pRIL carrying pet21b Dpb11 were induced overnight with 1mM IPTG at 24°C. Cells were lysed with a ball mill in 500mM NaCl, 50mM Tris pH 7.5, 0.1% NP-40, 10% glycerol, 2mM β -Me. Binding to NiNTA-agarose (Qiagen) occurred in the presence of 20mM imidazole and bound material was eluted with 1M imidazole. Further purification was carried out by gel filtration (Superdex 200) and cation exchange chromatography (Mono S).

GST-Dpb11 and fragments:

GST-Dpb11 and truncated versions were expressed in BL21 DE3 pRIL. Expression was induced overnight with 1mM IPTG at 24°C. Cells were lysed with a ball mill in 500mM NaCl, 50mM Tris pH 7.5, 0.1% NP-40, 10% glycerol, 2mM β -Me. For small scale (2 litre culture or less) cells were lysed with lysozyme (1mg/ml) and additional sonication. GST-tagged proteins were bound to Glutathione Sepharose 4B beads (GE Healthcare) and eluted with buffer containing 20mM glutathione. Further purification was carried out by cation exchange chromatography (Mono S).

MBP-Rad9 and mutants:

MBP-Dpb11 and corresponding versions were expressed in BL21 DE3 pRIL. Expression was induced overnight with 1mM IPTG at 24°C. Cells were lysed with a ball mill in 500mM NaCl, 50mM Tris pH 7.5, 0.1% NP-40, 10% glycerol, 2mM β -Me. For small scale (2 litre culture or less) cells were lysed with lysozyme (1mg/ml) and additional sonication. MBP-tagged proteins were bound to amylose resin (NEB) and

eluted with buffer containing 50mM maltose. Further purification was carried out by anion exchange chromatography (Mono Q).

Mec1-18myc-Ddc2:

YLL447.32/1A expressing an internally 18-myc tagged version of Mec1 was grown in a fermenter at 30°C up to a density of 1×10^8 cells. Cells were resuspended in 0.5 pellet volume of lysis-buffer (100mM KOAc, 25mM Hepes pH 7.6, 0.02% NP-40, 10% glycerol, 2mM β -Me, 10mM NaF, 20mM β -glycerophosphate, 100 μ M okadaic acid, protease inhibitors), frozen drop-wise in liquid nitrogen and lysed using a freezer mill. KOAc was added to a final concentration of 200mM and Hepes pH7.6 to 50mM. Lysates were cleared by two sequential steps of centrifugation (1h in 45Ti-rotor at 40000rpm). For each kinase assay 500 μ l of Mec1-18myc-Ddc2 containing extract was bound to 10 μ l 9E10 agarose (Santa Cruz). The bound material was washed twice in lysis buffer, once in lysis-buffer additionally containing 500mM LiCl and twice in kinase buffer (100mM KAc, 10mM Hepes pH 7.6, 50mM β -glycerophosphate, 10mM MgCl₂, 10% glycerol, 2mM β -Me).

Supplementary Figure Legends

Supplementary Figure 1.

The physical interaction of Dpb11 and Mec1-Ddc2 is constitutive.

(A) Unphosphorylated Mec1-Ddc2 can interact with Dpb11. GST-Dpb11 C (556-C) was immobilized on beads and used for pulldown of Ddc2-9myc. Cell extracts were dephosphorylated with λ -phosphatase (1200u per 100 μ l cell extracts (total protein concentration: 10-15mg/ml) for 30' at 30°C) before Dpb11-beads were added. Anti-myc westerns were used to detect Ddc2-9myc, Ponceau S staining to visualize GST-Dpb11 C.

(B) Mec1-Ddc2 interacts with Dpb11 independently of the cell cycle. Cells were released synchronously from alpha-factor arrest and three samples taken after 0', 30' and 60'. Cell extracts of these samples were used for pulldown using His-Dpb11 immobilized on NiNTA-agarose. Replication profiles were obtained by propidium iodide staining and FACS (lower panel).

(C) Mec1-Ddc2 binding to Dpb11 is not induced by DNA damage. Logarithmically growing cells were treated with 0.1% MMS for 2 h or left untreated as control. Cell extracts were prepared that contain Ddc2-9myc and interaction with His-Dpb11 bound to Ni-NTA-agarose was tested.

Supplementary Figure 2.

The C-terminal domain of Dpb11 controls the interaction with Mec1-Ddc2 and checkpoint signalling by two conserved W/YG motifs.

(A) The DNA damage checkpoint is defective in *dot1 Δ dpb11 Δ C* cells. *WT*, *dot1 Δ* , *dpb11 Δ C*, *dot1 Δ dpb11 Δ C* and *rad9 Δ* mutants were arrested with nocodazole and

treated with phleomycin (50 μ g/ml). Samples were taken after 15', 30', 45', 60' and 90' and checkpoint activation tested by the phosphorylation-dependent shift of Rad53.

(B) Sequence alignment of different vertebrate ATR activation domains (AAD) and C-termini of Dpb11 orthologues from different fungi: scerDpb11 = *Saccharomyces cerevisiae* DPB11/YJL090C, scasDpb11 = *Saccharomyces castellii* WashU_Scas_Contig711.30, sparDpb11 = *Saccharomyces paradoxus* MIT_Spar_c341_11622, sbayDpb11 = *Saccharomyces bayanus* MIT_Sbay_c722_12730, skudDpb11 = *Saccharomyces kudriavzevii* WashU_Skud_Contig1640.2, klacDpb11 = *Kluyveromyces lactis* KLLA0F14300g, agosDpb11 = *ashbya gossypii* AGOS_AFR095, pstiDpb11 = *Pichia stipitis* PICST_83141, spomCut5 = *Schizosaccharomyces pombe* CUT5 yspCUT5, xlTopBP1 = *Xenopus laevis* TopBP1, Cut5 related protein (AB091779.1), ggTopBP1 = *Gallus gallus* TopBP1 (XM_418794.2), hsTopBP1 = *Homo sapiens* TopBP1 (NM_007027.3). Grey arrows indicate the position of the W/YG motifs that are homologous to *DPB11* WG700,701 and YG735,736 in Dpb11 orthologues from different fungi, a black arrow indicates the position of TopBP1 W1145.

(C-D) The checkpoint defect of *dpb11 Δ C dot1 Δ* mutants is weaker compared to *dpb11-1 dot1 Δ* . **(C)** Rad53-phosphorylation was measured as in (A), but cells were grown at 25°C (permissive temperature for *dpb11-1*) and treated with 50 μ g/ml phleomycin for 30' (+). **(D)** To test for survival cells were released from nocodazole arrest concomitantly with addition of phleomycin. Cells were plated in serial dilution before and 1h and 2h after addition of phleomycin.

(E) Mutation of any W/YG motif abrogates the Dpb11-Mec1-Ddc2 interaction. Indicated mutations were introduced into GST-Dpb11 C (556-C). WT and mutant

proteins were expressed in *E. coli*, purified, bound to Glutathione-sepharose and used to pull down Ddc2-9myc from cell extracts. Ddc2-9myc was detected by myc-western, GST-Dpb11 C fusion proteins by Ponceau S staining.

(F) Mutation of the WG-motif phenocopies *dpb11ΔC*. The *dpb11 WG700,701AA* was ectopically expressed under control of the endogenous promoter in a *dpb11Δ* background. Cells were arrested with nocodazole and treated with 50μg/ml phleomycin for 30'. Checkpoint activation was as in (a).

Supplementary Figure 3.

Phosphorylated Serine 462 and Threonine 474 are bound by the N-terminus of Dpb11.

(A) 35mer peptides were generated corresponding to the amino acid sequence of putative CDK sites of Rad9. They harbour the indicated phosphorylated amino acid at position 26 (with the exception of S11, which is at position 11) and are N-terminally tagged with an EAhx-linker and a biotin moiety. For pulldown they were immobilized on Streptavidin-coupled Dynabeads. To control for phosphospecificity half of the beads were treated with λ-phosphatase, while the other half was mock treated. Binding of GST-Dpb11 N (aa 1-276) to peptide beads was tested by pulldown. The Dpb11 BRCT I+II interacting peptide from Sld3 served as a positive control (Zegerman and Diffley, 2007). In the upper domain diagram of Rad9 the position of the 20 S/TP motifs is shown: sequence conservation in *Saccharomyces sensu lato* is indicated by green, the four non-conserved sites are marked in white. In the lower diagram Dpb11-binding peptides are indicated in orange, non-binding sequences in green and sequences that were not tested in white.

(B) The peptide containing S462 requires phosphorylation for binding to Dpb11. Procedure as in (A), but instead of phosphatase treatment a non-phosphorylated peptide, which is otherwise identical to the S462-peptide, was used. As a negative control the S507-phosphopeptide was chosen. Sld3 positive control as in (A).

Supplementary Figure 4.

Rad9-phosphorylation-specific antibodies site-specifically recognize MBP-Rad9 phosphorylated by Cdk *in vitro*. Recombinant MBP-Rad9, MBP-Rad9 S462A and MBP-Rad9 T474A were phosphorylated to completion *in vitro* with mammalian Cyclin A Δ N170-Cdk2 or left untreated. A polyclonal anti-Rad9 antibody and the phospho-S462- and phospho-T474-specific antibodies were used in Western blots.

Supplementary Figure 5.

Similarity of the primary sequence of the CDK-dependent Dpb11 interaction sites in Rad9 and Sld3 and evolutionary conservation of these sites in Rad9 orthologues from different fungi.

(A) Alignment of the primary sequence surrounding S462 and T474 in Rad9 orthologues of *Saccharomyces sensu lato*, and the sequences surrounding T600 and S622 in Sld3 orthologues. Shown are amino acid sections of the following sequences: ScerRad9 = *Saccharomyces cerevisiae* Rad9, YDR217c, SbayRad9 = *Saccharomyces bayanus* MIT_Sbay_c498_4535, SparRad9 = *Saccharomyces paradoxus* MIT_Spar_c118_4555, SkudRad9 = *Saccharomyces kudriavzevii* WashU_Skud_Contig1811.1, ScasRad9 = *Saccharomyces castellii* WashU_Scas_Contig721.91, ScerSld3 = *Saccharomyces cerevisiae* Sld3, YGL113w, SbaySld3 = *Saccharomyces bayanus* MIT_Sbay_c393_8133, SparSld3 =

Saccharomyces paradoxus MIT_Spar_c22_8756, SkudSld3 = *Saccharomyces kudriavzevii* WashU_Skud_Contig2026.5, ScasSld3 = *Saccharomyces castellii* WashU_Scas_Contig652.4. Grey arrows indicate the position of S462 and T474 of *Saccharomyces cerevisiae* Rad9 (top) and of T600 and S622 of *Saccharomyces cerevisiae* Sld3 (bottom).

(B) Domain diagram of Rad9 homologues: scRad9 = *Saccharomyces cerevisiae* Rad9, YDR217c, spCrb2 = *Schizosaccharomyces pombe* Crb2 BAA13093, hs53bp1 = *Homo sapiens* 53bp1. Positions of S/TP motifs are indicated by green dots, positions of S/TQ motifs are indicated by orange dots. Domain borders of TUDOR and BRCT domains were derived from published alignments (Kilkenny et al., 2008; Lancelot et al., 2007).

(C) Evolutionary conservation of Rad9 S462 and T474 CDK sites in different fungi. Shown is the CDK site containing part of a sequence alignment of different fungal Rad9 homologues: ScerRad9 = *Saccharomyces cerevisiae* Rad9, YDR217c, SbayRad9 = *Saccharomyces bayanus* MIT_Sbay_c498_4535, SparRad9 = *Saccharomyces paradoxus* MIT_Spar_c118_4555, SkudRad9 = *Saccharomyces kudriavzevii* WashU_Skud_Contig1811.1, ScasRad9 = *Saccharomyces castellii* WashU_Scas_Contig721.91, AgosRad9 = *Ashbya gossypii* AGOS_AGR173C, KlacRad9 = *Kluyveromyces lactis* KLLA0F13068g, PstiRad9 = *Pichia stiptis* PICST_32199, AnigRad9 = *Aspergillus niger* An09g06150 XP_001393927, SpomCrb2 = *Schizosaccharomyces pombe* Crb2 BAA13093. Grey arrows indicate the position of S462 and T474 in *Saccharomyces cerevisiae* Rad9. For *Schizosaccharomyces pombe* Crb2 S226 (underlined) and T235 are potential candidate sites, to mediate CDK-dependent interaction with Cut5, but S226 might be too close to T215.

Supplementary Figure 6.

Genetic Analysis of the CDK-phosphorylation site mutant *rad9 ST462,474AA*.

(A) Epistasis analysis suggests that the Rad9-Dpb11 interaction, which is abrogated by the *rad9 ST462,474AA* mutation, interaction is functionally dependent on the 9-1-1-Dpb11 interaction, which is defective in the *ddc1 T602A* mutant. *rad9 ST462,474AA* and *ddc1 T602A* single and double mutants in the background of *DOT1* or *dot1Δ* were arrested with nocodazole and checkpoint activation after phleomycin-treatment (50 μg/ml; left panel: 30', right panel: indicated time) was determined by Rad53-western blot and testing of cellular survival. *ddc1 T602A* in the absence or presence of *DOT1* (lane 4 or 3) has a slightly stronger phenotype compared to the corresponding *rad9 ST462,474AA* strains (lane 6 or 5) and importantly the *rad9 ST462,474AA ddc1 T602A* double mutant does not lead to further increase in the checkpoint defect (lane 8 or 7).

(B) CDK-phosphorylation of Rad9 is not required for DNA damage induced phosphorylation of Dpb11. *WT*, *rad9 ST462,474AA* and *ddc1 T602A* strains were treated as in (A). DNA-damage dependent phospho-shift of Dpb11 was detected in anti-Dpb11-C western. Dpb11-phosphorylation depends on Mec1 and a functional 9-1-1-Dpb11 interaction (Puddu et al., 2008). This suggests that modification requires correct localization of Dpb11 to DNA damage sites. Since Dpb11 phosphorylation is similar in *WT* and *rad9 ST462,474AA* cells, the Rad9-Dpb11 appears not to be involved in the recruitment of Dpb11 to DNA damage sites. The asterisks label crossreactive bands.

(C) The G2/M DNA damage checkpoint is affected similarly by *rad9 ST462,474AA* and *dpb11ΔC* mutations, but mutants have a non-epistatic relationship. *WT*, *dot1Δ*,

rad9 ST462,474AA and *dpb11ΔC* strains and double and triple mutant combinations were treated as in (A). The *rad9 ST462,474AA dpb11ΔC dot1Δ* triple mutant (lane 8) has a slightly stronger phenotype compared with *dpb11ΔC dot1Δ* (lane 4) and *rad9 ST462,474AA dot1Δ* (lane 6) double mutants. This suggests that both Rad9-Dpb11-9-1-1 and 9-1-1-Dpb11-Mec1-Ddc2 subcomplexes are partially functional in the mutant complex. In WT cells a full ternary complex may be required for efficient checkpoint activation.

Supplementary Figure 7.

Covalent fusion of Rad9 and Dpb11 creates a gain-of-function mutant that causes checkpoint hyperactivation, but does not interfere with the replication function of Dpb11.

(A) Cells expressing the *RAD9 AA-DPB11ΔN*-fusion protein replicate DNA with wild-type kinetics. WT cells or cells in which the *RAD9 AA-DPB11ΔN* fusion was ectopically expressed from the *DPB11* promoter as only cellular copy of *RAD9* were synchronously released from G1 arrest (α). DNA content of fixed cells was measured by SYTOX Green staining and FACS. Asynchronously dividing cells (asy) are shown as control.

(B) The *RAD9 AA-DPB11ΔN*-fusion dominantly leads to checkpoint hyperactivation. WT cells or cells expressing *RAD9 AA-DPB11ΔN* from the *DPB11* promoter in the presence or absence of endogenous *RAD9* were arrested in G2/M using nocodazole and treated with 1.5, 5, 15 or 50 μ g/ml phleomycin for 30'. Checkpoint activation was tested by the phospho-shift of Rad53. At low doses of phleomycin the *RAD9 AA-DPB11ΔN*-fusion leads to increased Rad53 phosphorylation. The *RAD9 AA-*

DPB11ΔN is dominant over endogenous Rad9 indicative of a gain-of-function mutation.

(C) The *RAD9 AA-DPB11ΔNΔC*, but not *RAD9 AA-DPB11ΔN* is inactive, when the 9-1-1-Dpb11 interaction is inhibited by the *ddc1 T602A* mutation. *RAD9 AA-DPB11ΔN* (276-C) or *RAD9 AA-DPB11ΔNΔC* (276-600) were ectopically expressed from the *DPB11* promoter as only cellular copy of *RAD9* in *WT*, *dot1Δ* or *dot1Δ ddc1 T602A* strains. G1 arrested cells were treated with 50μg/ml phleomycin for 30' (+) and checkpoint activation was assayed by Rad53 western blot. When Rad9 and Dpb11ΔN are fused cells show a different requirement for the 9-1-1-Dpb11 interaction compared to cells expressing WT Dpb11 (Figure 2G-H). This suggests that *RAD9 AA-DPB11ΔN*-fusion cells have acquired an additional way to recruit Dpb11 to DNA damage sites. Since additional truncation of the DPB11 C-terminus renders the checkpoint defective, this additional pathway depends on the C-terminal Mec1-Ddc2 interaction domain. Moreover, although Dpb11ΔC is unable to activate Rad53 in the absence of Dot1 (Figure 2C-D), the *RAD9-AA-DPB11ΔNΔC* fusion is able to efficiently activate Rad53. This function is however abolished in the *ddc1 T062A* mutant.

(D) The *RAD9 AA-DPB11ΔN* fusion leads to prolonged checkpoint signalling. Strains as in (A) were arrested with nocodazole and treated with 15 or 50μg/ml phleomycin for 30'. Phleomycin was washed away and cells were released in medium containing nocodazole but no phleomycin. Samples were taken at the indicated timepoints after release and checkpoint activity tested as in (A).

Supplementary Figure 8.

Phosphorylation of Rad9 by Mec1 is enhanced in a ternary Rad9-Dpb11-Mec1-Ddc2 complex.

(A) Pre-phosphorylation of Rad9 with recombinant CDK. Purified MBP-Rad9 or MBP-Rad9 ST462,474AA were phosphorylated with CDK (btCyclin A Δ N170-hsCdk2) *in vitro*. Removal of CDK was achieved by binding of MBP-Rad9 to amylose beads and elution with maltose. This fraction was then used as a substrate in the Mec1 kinase assays in Fig. 5b-c and Sup. Fig. 8b-d.

(B) Confirmation of the Rad9-phosphorylation signal after incubation by Mec1. An MBP-TEV version of Rad9 (0.7pmol) was used as a substrate in a kinase assay with immunopurified, bead-immobilized Mec1-Ddc2 and Dpb11 (0.75 pmol). TEV protease was added to the kinase assay, resulting in a downshift of the Rad9 containing bands.

(C) Titration of the activator (Dpb11) in Mec1-kinase assays of Rad9. Kinase assay as in (B) but the amounts of GST-Dpb11 or GST-Dpb11 C were titrated (0.075, 0.25, 0.75pmol). Quantification of the Rad9 western blot showed that 1.4fold more MBP-Rad9 were used compared MBP-Rad9 ST462,474AA. Therefore approximately 0.45pmol WT Rad9 and 0.3pmol Rad9 ST462,474AA were used as substrate in this assay.

(D) Substrate titration (Rad9) in Dpb11-dependent Mec1-kinase assays. Kinase assay as in (B) but with 0.75pmol GST-Dpb11 or GST-Dpb11 C. Further, MPB-Rad9 or MBP-Rad9 ST462,474AA was used as a substrate and titrated (0.15, 0.5, 1.5pmol).

Supplementary Figure 9.

Influence of Mec1-activating proteins on DNA damage checkpoint signalling.

(A) Rad9-phosphorylation by Mec1 *in vivo* is dependent on the CDK-induced Rad9-Dpb11 interaction, but to a lesser extent on Mec1 activation by Dpb11. *RAD9-3Flag* or *RAD9 ST462,474AA-3Flag* were expressed as the only copy of *RAD9* in *WT*, *dot1Δ*, *dpb11ΔC* or *dot1 dpb11ΔC* mutant backgrounds. Nocodazole arrested cells were treated with 50μg/ml phleomycin for 30' (+). Phosphorylated species of Rad9-3Flag can be seen in anti-Flag western blot: CDK phosphorylated Rad9 (CDK-P) shows an intermediate upshift and Rad9 phosphorylated by Mec1 (SQ-P) shows a large shift in electrophoretic mobility after DNA damage induction.

(B) Combination of mutants of both known Mec1 activators leads to a defect in checkpoint activation. *WT*, *dot1Δ*, *dpb11ΔC*, *ddc1 WW352,544A*, the corresponding double mutants and the *dot1Δ dpb11ΔC ddc1 WW352,544A* triple mutant strains were tested for their ability to activate the G2/M DNA damage checkpoint. Cells were grown in minimal medium lacking tryptophan in order to maintain pRS314 constructs, arrested with nocodazole and treated with 50μg/ml phleomycin for 30' or 60'. Checkpoint activation was indicated by phosphorylation of Rad53 (left panel). For testing of cellular survival cells were released from the nocodazole block concomitant with the phleomycin treatment. Serial dilutions of cells before and 1h or 2h after addition were spotted on plates not containing drugs and incubated for 2 days at 30°C (right panel).

Supplementary Figure 10.

A partial Dpb11 pathway is active in G1 under conditions of high DNA damage. This pathway depends on the interactions of Dpb11 with the 9-1-1 complex and Mec1-

Ddc2, but is independent of CDK phosphorylation of Rad9. Accordingly it is fully supported by a version of Dpb11, which lacks the N-terminal BRCT 1+II domain.

(A) Residual DPB11-dependent checkpoint activation can be observed in G1-arrested *dot1Δ* cells treated with a high dose of phleomycin (200μg/ml). *dot1Δ* single mutant strains and double mutant combinations with *dpb11ΔC*, *ddc1 T602A* and *rad9 ST462,474AA* were arrested with alpha-factor (left panel) or nocodazole (right panel) and tested for checkpoint activation (Rad53 phosphorylation) in the presence of 50μg/ml and 200μg/ml phleomycin. The residual checkpoint response in G1 arrested *dot1Δ* mutants depends on Dpb11 interactions with the 9-1-1 complex and Mec1-Ddc2 and can also be seen in G2/M arrested *dot1Δ rad9 ST462,474AA* mutants. The physiological significance of this response is unclear – WT cells will show a complete upshift of Rad53 to the phosphorylated form even at lower doses of phleomycin (compare to figure 4A).

(B) Dpb11ΔN fully supports Rad9-CDK-phosphorylation-independent Dpb11 functions in G1, indicating that Dpb11ΔN can functionally interact with Ddc1 and Mec1-Ddc2. Full length Dpb11 or Dpb11ΔN were expressed in the *dot1Δ dpb11ΔC* and checkpoint function was assayed in G1 arrested cells as in (A). Expression of different versions of Dpb11 was tested in an anti-Dpb11 C western blot.

Supplementary Figure 11.

The BRCT repeat I mutant *dpb11 T12A* does not rescue the checkpoint defect of *dpb11ΔC dot1Δ*.

(A) *dpb11 T12A* is unable to support viability indicative of defective replication. This indicates that BRCTI+II function is abolished by the *T12A* mutation. The *dpb11 T12A* allele was ectopically expressed from the *TRP1* locus under control of the *DPB11*

promoter. When heterozygous *dpb11Δ* diploids carrying this mutant version of *DPB11* as a second copy were sporulated, *dpb11 T12A* failed to rescue the *dpb11Δ* knock-out, as seen by 2+2 segregation of viable spores.

(B) Similar to *dpb11ΔN*, *dpb11 T12A* fails to rescue the checkpoint defect of *dpb11ΔC dot1Δ*. *Dpb11 T12A*, *Dpb11ΔN* and *Dpb11* were expressed as a second copy of *DPB11* in *dot1 dpb11ΔC* strains. Cells were arrested with nocodazole and treated with 50μg/ml phleomycin for 30'. Checkpoint activation was tested by the phosphorylation-dependent shift of Rad53. (left panel). Expression of different versions of *Dpb11* was verified by western blotting using an antibody directed against the C-terminus of *Dpb11*. For test of cellular survival cells were released from the nocodazole block concomitant with the phleomycin treatment. Serial dilutions of cells before and 1h or 2h after addition were spotted on plates not containing drugs and incubated for 2 days at 30°C (right panel).

Supplementary citations:

de la Torre-Ruiz, M.A., Green, C.M., and Lowndes, N.F. (1998). RAD9 and RAD24 define two additive, interacting branches of the DNA damage checkpoint pathway in budding yeast normally required for Rad53 modification and activation. *EMBO J* 17, 2687-2698.

James, P., Halladay, J., and Craig, E.A. (1996). Genomic libraries and a host strain designed for highly efficient two-hybrid selection in yeast. *Genetics* 144, 1425-1436.

Kilkenny, M.L., Dore, A.S., Roe, S.M., Nestoras, K., Ho, J.C., Watts, F.Z., and Pearl, L.H. (2008). Structural and functional analysis of the Crb2-BRCT2 domain reveals distinct roles in checkpoint signalling and DNA damage repair. *Genes Dev* 22, 2034-2047.

Lancelot, N., Charier, G., Couprie, J., Duband-Goulet, I., Alpha-Bazin, B., Quemeneur, E., Ma, E., Marsolier-Kergoat, M.C., Ropars, V., Charbonnier, J.B., *et al.* (2007). The checkpoint *Saccharomyces cerevisiae* Rad9 protein contains a tandem tudor domain that recognizes DNA. *Nucleic Acids Res* 35, 5898-5912.

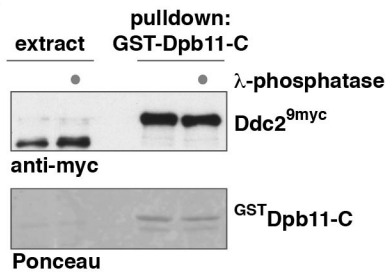
Paciotti, V., Clerici, M., Lucchini, G., and Longhese, M.P. (2000). The checkpoint protein Ddc2, functionally related to *S. pombe* Rad26, interacts with Mec1 and is regulated by Mec1-dependent phosphorylation in budding yeast. *Genes Dev* 14, 2046-2059.

Puddu, F., Granata, M., Di Nola, L., Balestrini, A., Piergiovanni, G., Lazzaro, F., Giannattasio, M., Plevani, P., and Muzi-Falconi, M. (2008). Phosphorylation of the budding yeast 9-1-1 complex is required for Dpb11 function in the full activation of the UV-induced DNA damage checkpoint. *Mol Cell Biol* 28, 4782-4793.

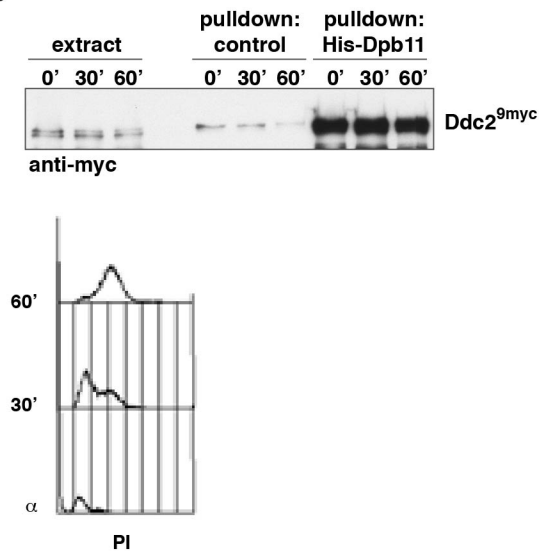
Rothstein, R.J. (1983). One-step gene disruption in yeast. *Methods Enzymol* 101, 202-211.

Zegerman, P., and Diffley, J.F. (2007). Phosphorylation of Sld2 and Sld3 by cyclin-dependent kinases promotes DNA replication in budding yeast. *Nature* 445, 281-285.

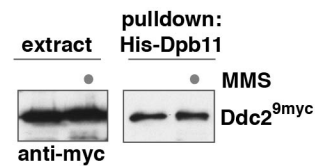
A



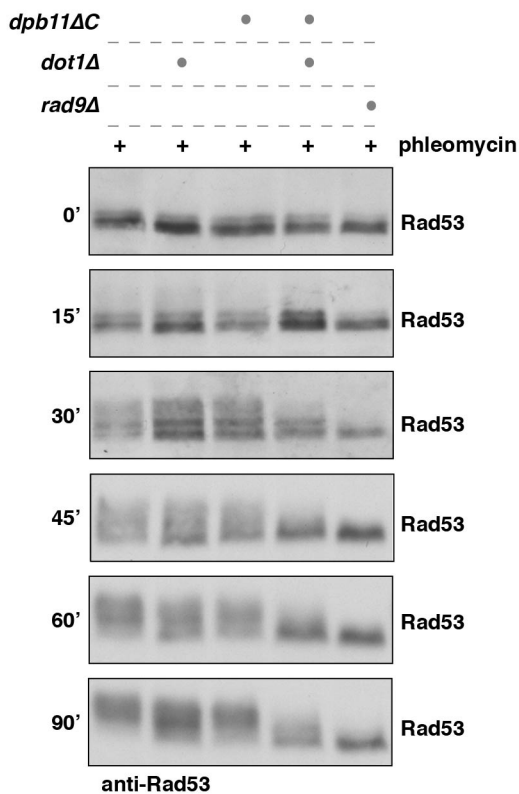
B



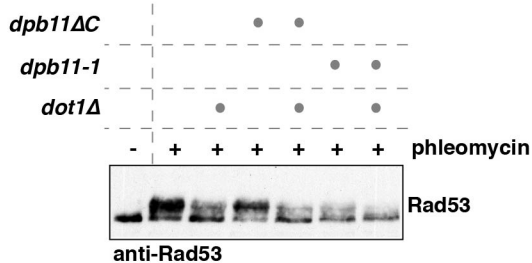
C



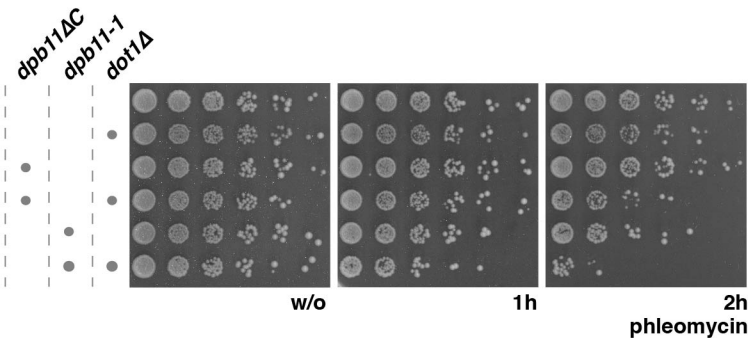
A



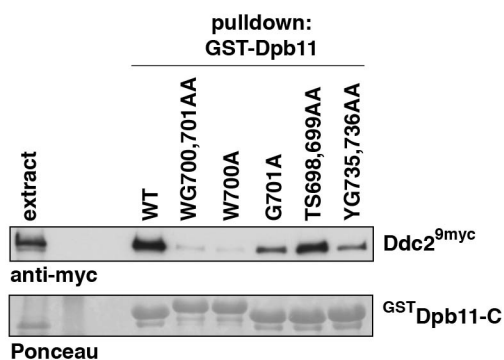
C



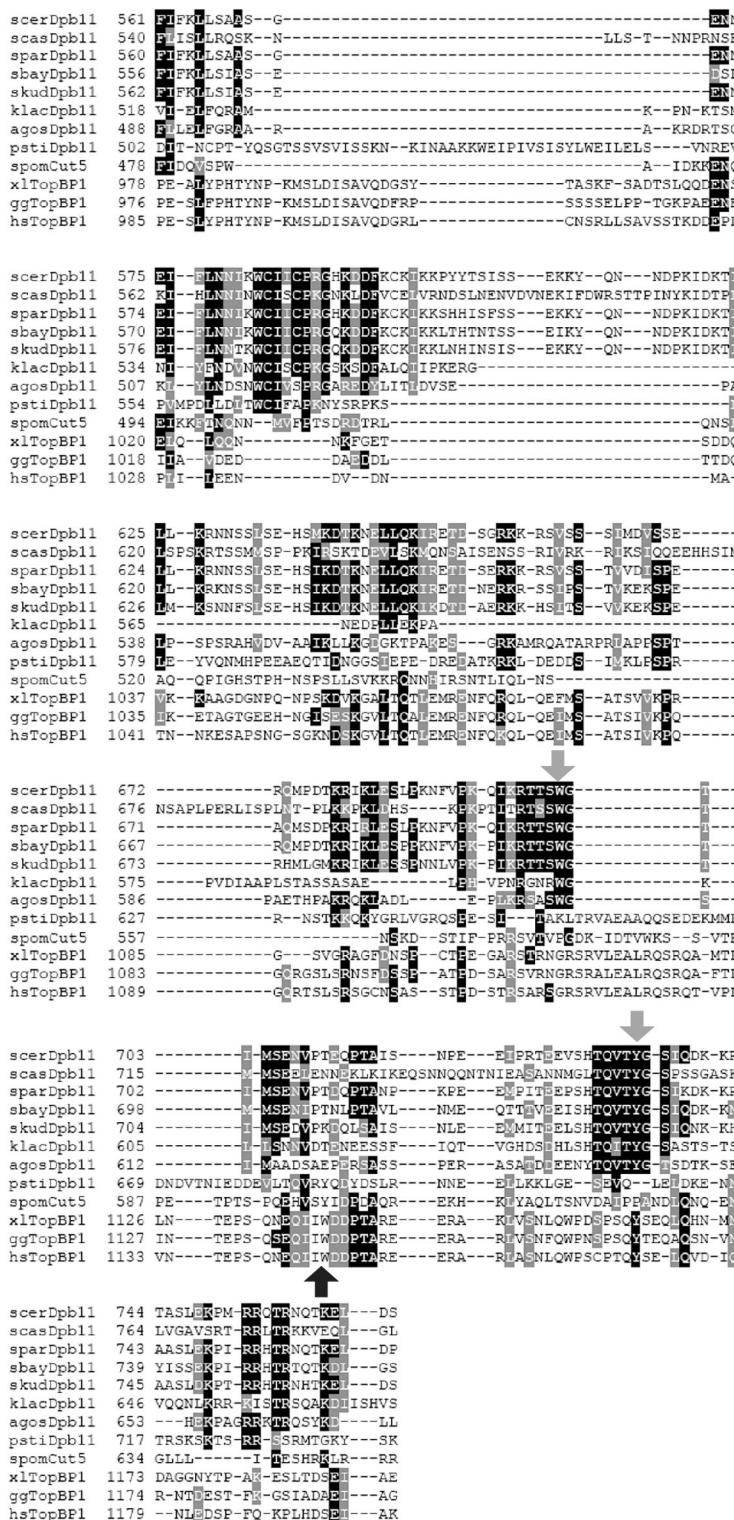
D



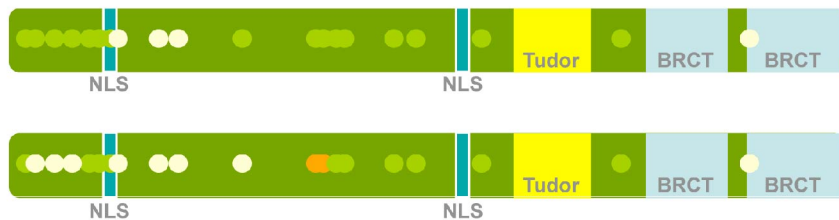
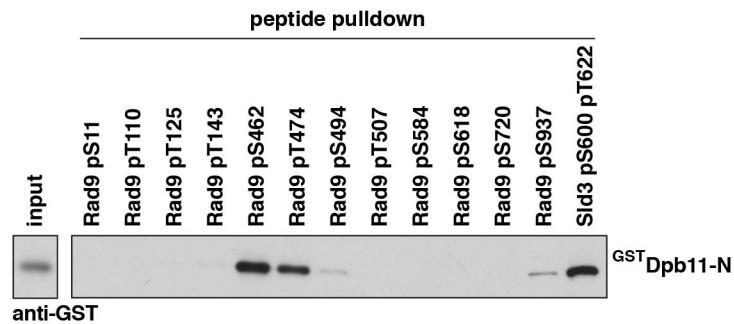
E



B



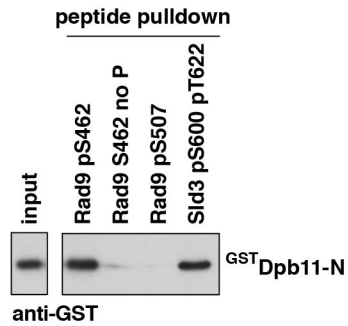
A

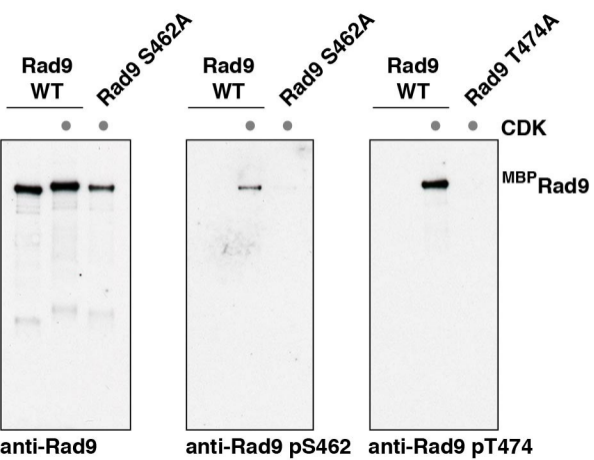


- SP/TP site conserved in *Sacharomyces sensu lato*
- SP/TP site not conserved in *Sacharomyces sensu lato*

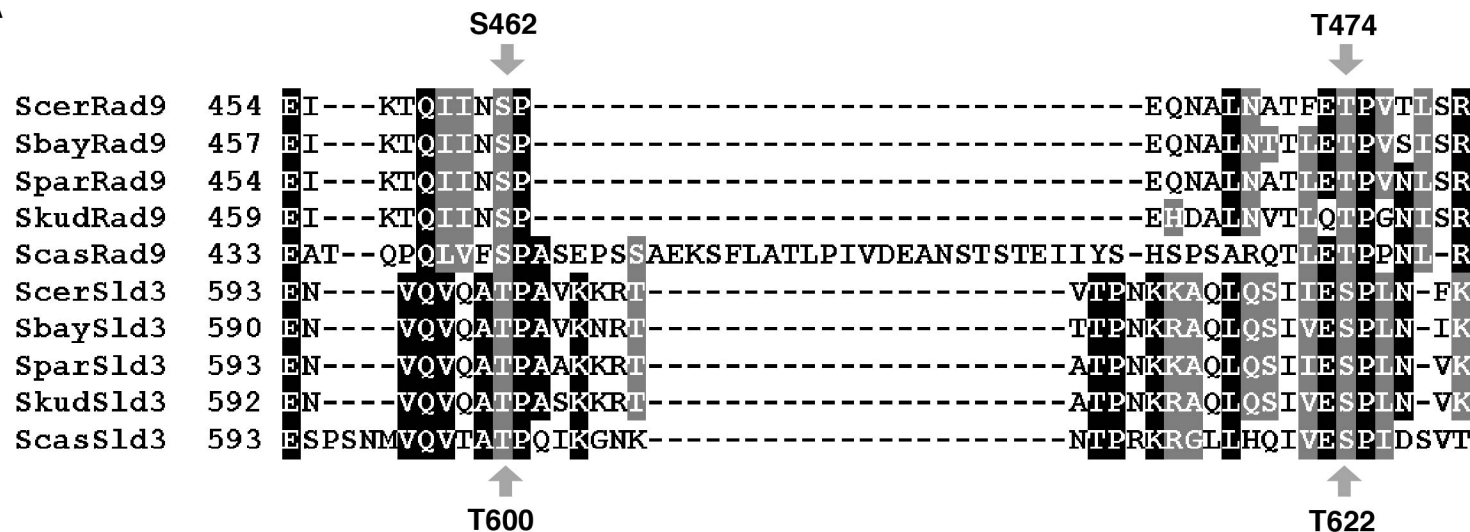
- SP/TP peptide did not show binding to Dpb11
- SP/TP peptide not tested for binding to Dpb11
- SP/TP peptide shows binding to Dpb11

B

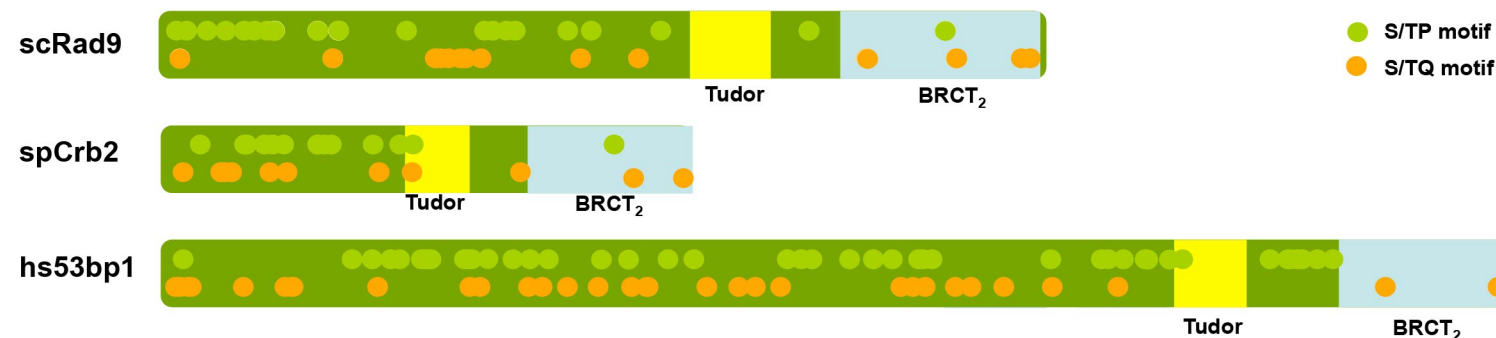




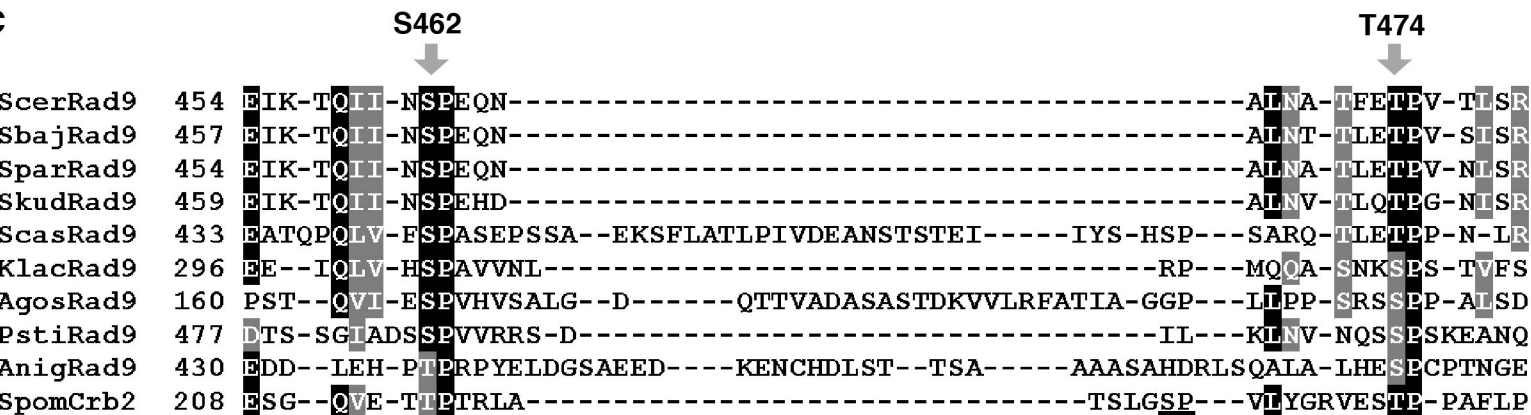
A



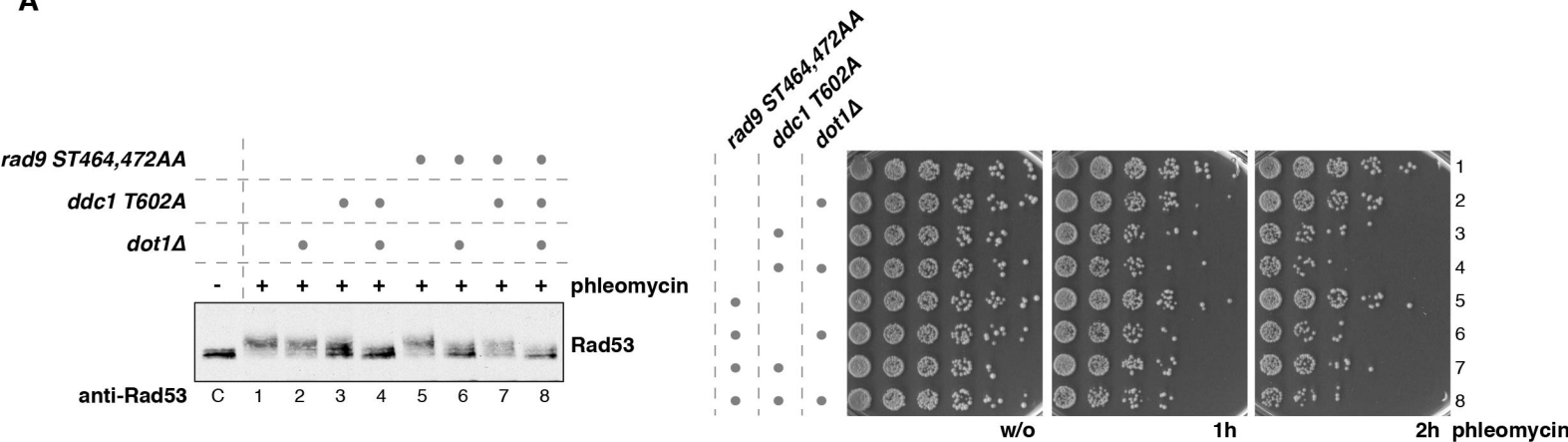
B



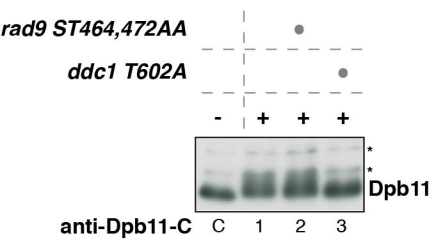
C



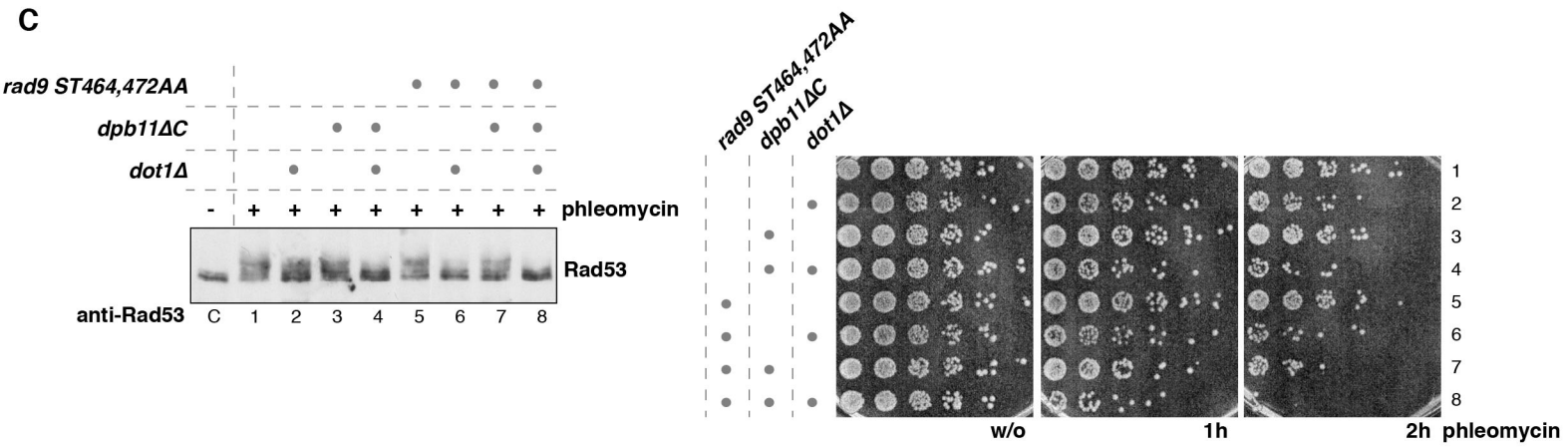
A



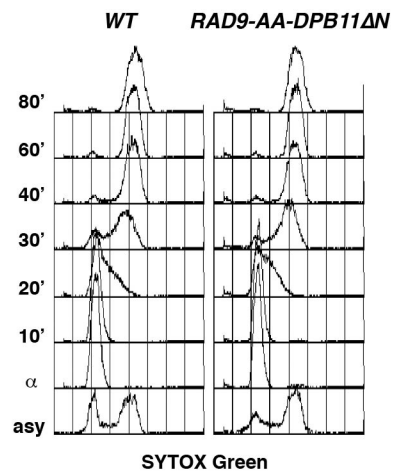
B



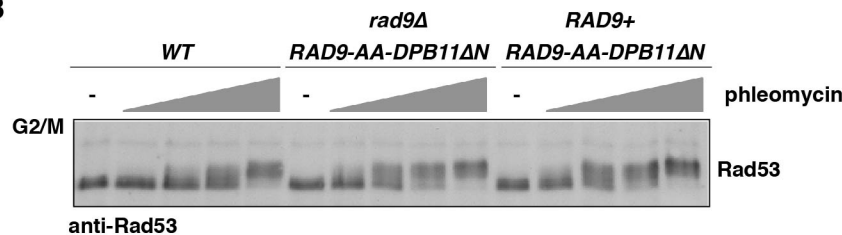
C



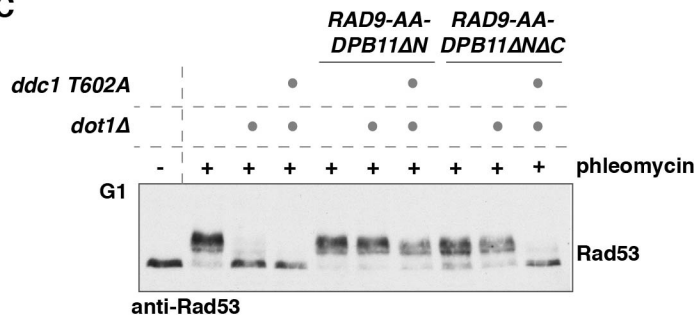
A



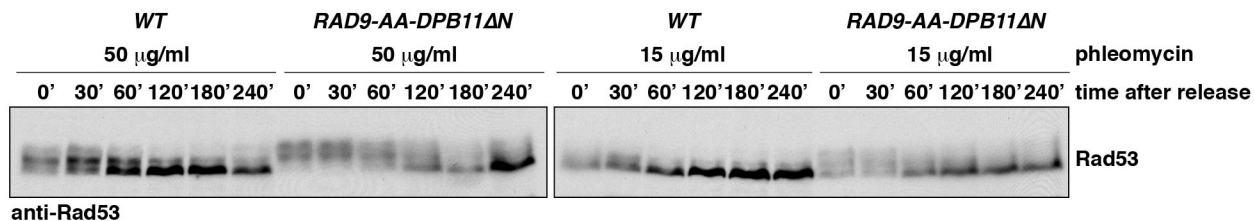
B



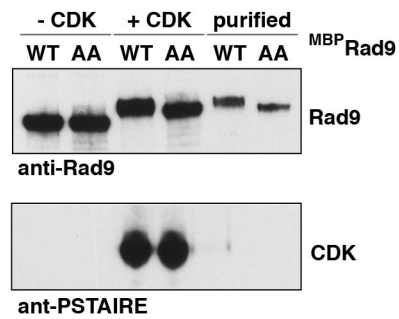
C



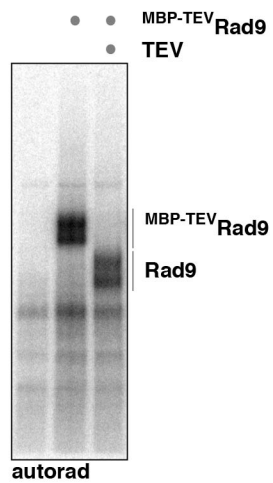
D



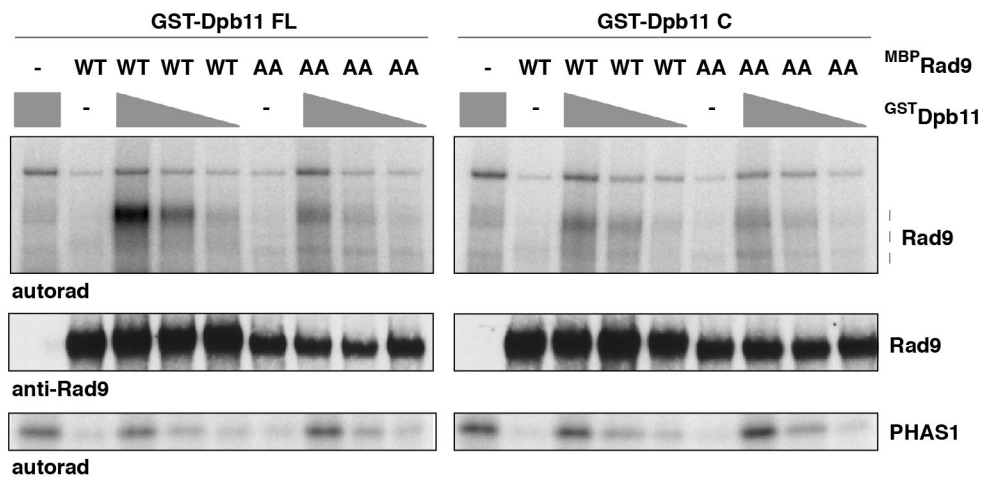
A



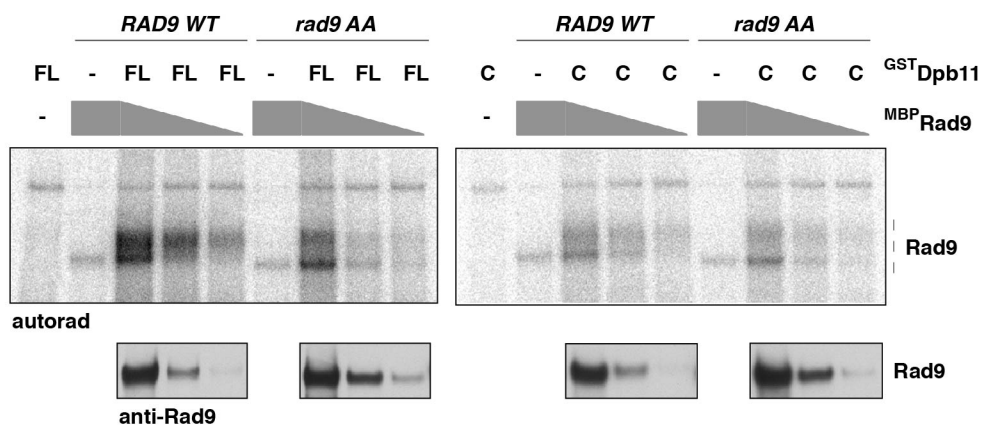
B



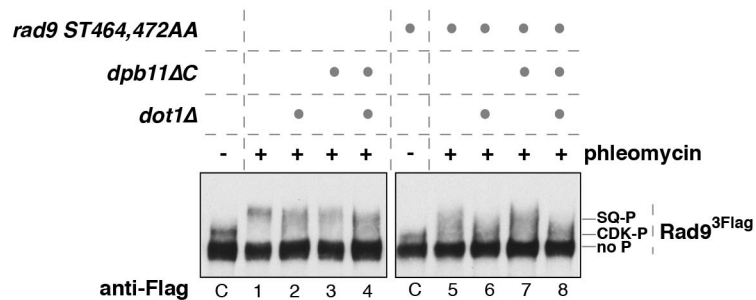
C



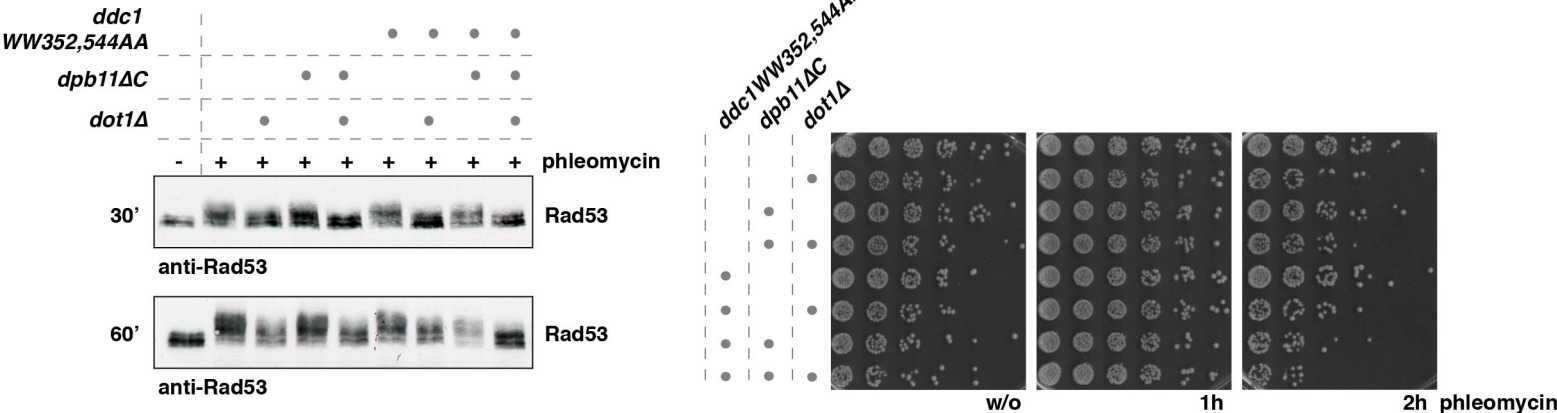
D



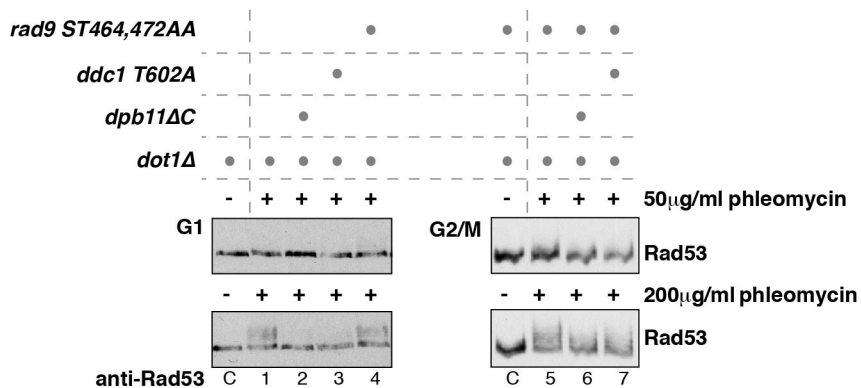
A



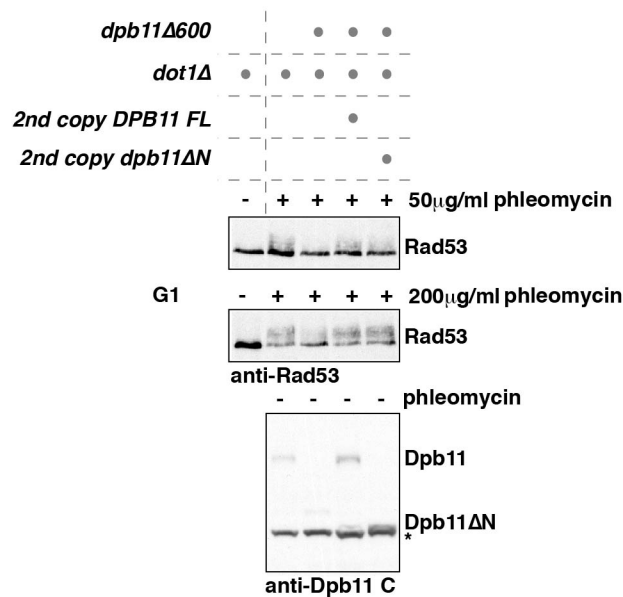
B



A



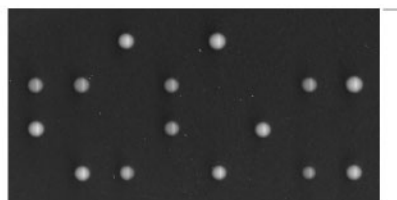
B



A

spore analysis
dpb11Δ dpb11 T12A::TRP1

DPB11 TRP1



spores originating
 from one tetrad

B

